IEEE Access
Multidisciplinary | Rapid Review | Open Access Journal

Received 10 August 2023, accepted 9 September 2023, date of publication 22 September 2023,
date of current version 27 September 2023.

Digital Object Identifier 10.1109/ACCESS.2023.3318108

RESEARCH ARTICLE

A TV-MPC Methodology for Uncertain Under-Actuated Systems: A Rotary Inverted Pendulum Case Study

FARRUKH WAHEED[1,2], IMRAN KHAN YOUSUFZAI[3], AND MICHAEL VALÁŠEK[1]

[1]Faculty of Mechanical Engineering, Czech Technical University in Prague, 166 07 Prague, Czech Republic
[2]Department of Electronics and Software, Institute of Experimental and Applied Physics (IEAP), Czech Technical University in Prague, 110 00 Prague, Czech Republic
[3]Department of Electrical, Electronics and Computer Systems Engineering, College of Engineering and Technology, University of Sargodha, Sargodha 40100, Pakistan

Corresponding author: Imran Khan Yousufzai (imran.khan@uos.edu.pk)

This work was supported in part by Czech Technical University (CTU) in Prague, Czech Republic, through Student Grant Competition (SGS) for the project "Modeling, control and design of mechanical systems 2016" and for the project "Modeling, control and design of mechanical systems 2019" under Grant SGS16/209/OHK2/3T/12 and Grant SGS19/157/OHK2/3T/12; in part by the Department of Electrical Engineering, University of Sargodha (UOS), Pakistan; and in part by the Automatic Control and System Dynamics (ACSD) Laboratory, Technische Universitét Chemnitz, Germany.

ABSTRACT This paper presents a systematic approach of formulating a Time-Varying Model Predictive Control (TV-MPC) framework for uncertain and under-actuated mechanical systems. The proposed methodology utilizes the nonlinear decomposed dynamics in conjunction with a special class of orthonormal basis functions – the Laguerre functions in the model structure. A possible numerical ill-conditioning problem, for large prediction horizons, has been coped with using the idea of exponential data weighting in the cost function, which results in condition number improvement, for the main TV-MPC algorithm. A rotary inverted pendulum is considered as a case study under-actuated system. The content of this research revolves around the TV-MPC treatment for cubic polynomial type reference position tracking problem using the decomposed nonlinear dynamics in the TV-MPC model structure and using Laguerre functions for future control trajectory modeling and motion predictions of the rotary servo arm and the pendulum bar. Finally, the applicability of TV-MPC algorithm is demonstrated with the help of simulation results for the subject benchmark system.

INDEX TERMS Time-varying MPC (TV-MPC), orthonormal basis functions, Laguerre functions, numerical ill-conditioning, cubic polynomials, dynamic decomposition, under-actuated systems.

I. INTRODUCTION

Model Predictive Control (MPC), invented in the early 70's, is a methodical control approach which got popularity in the production industry by providing ease of handling complicated multi-variable dynamics. Its popularity was further strengthened by a built-in optimization routine which provided ease of handling *constraints* on controlled and/or manipulated variables [1]. The MPC has been deployed successfully in various applications ranging from process control [2], autonomous vehicles [3], robotics [4], economics and even in medical/health sciences [5]. Over the course of research, initiated by the novel industrial requirements and technological advancements, many variants of MPC were proposed i.e., hybrid MPC [6], tube MPC [7], stochastic MPC [8], learning Based (or data driven) MPC [9].

The core of an MPC algorithm is a model structure for prediction. Various approaches are popular for Predictive Control Design (PCD), each one having a unique model structure for the predictive control formulation.

The earlier formulations employed a Finite Impulse Response (FIR) or Step-Response (SR) models as prediction models. The Dynamic Matrix Control (DMC) formulation, proposed in 1979, is an example of FIR/SR model based MPC. These models gave better descriptions of process time delay, response time and gain. However, the algorithms based

The associate editor coordinating the review of this manuscript and approving it for publication was Xiwang Dong.

on these models are not computationally efficient since the underlying algorithm requires 30 to 60 impulse response coefficients (or even more) depending on the process type and the choice of sampling interval. Moreover, these formulations are applicable to stable plants only and such plant models might have large model orders depending on the process type.

The idea of transfer function based prediction models, in 1984, caused the emergence of Generalized MPC (GMPC) paradigm [10]. However, the transfer function based GMPC posed problems in multi-variable control applications and proved to be less effective in handling multi-variable plants (systems or processes). An advanced type of formulation, widely used in most of the PCD, is based on state-space models, initially presented in 1993 [11] and later on many other variants were proposed in [1], [12], [13], and [14]. A state-space based GMPC got attention as being more methodical and especially effective in multi-variable control environment.

Another feature of MPC (the optimality of solutions), classifies it into two categories from implementation perspective: Implicit and explicit. An optimal solution obtained by an iterative procedure is referred to as *implicit MPC* while evaluating the explicit representation of an MPC feedback law, which is obtained off-line using parametric programming is referred to as *explicit MPC*. Implicit MPC handled large systems but at the expense of computational efficiency. Explicit MPC, on the other hand, were computationally efficient, from implementation point of view, but are not a good option to be used for higher order systems. Whether an MPC is implicit or explicit, the researchers have proposed many solutions to come up with an optimal solution [15], [16], [17], [18], [19]. The modern day research uses continuous time approximations for predictive control model like Hammerstein models [20], [21], [22], Wiener models [23], [24], [25] and impulse response approximation (set of orthonormal functions [26], [27], [28], [29], [30], [31], [32], [33], [34], usually ''Laguerre Model'', see [28]). The orthonormal functions approach to control trajectory modeling guaranteed bounded Integral Square Value (ISV) that is L^2 stable.

On the other hand, stabilization of rotary inverted pendulum poses a variety of control challenges. The usual ones include the under-actuated nature, open loop instability and coupled nonlinear dynamics. Many real-world problems can better be prototyped by using this simple test bench apparatus. For example, the attitude control of a booster rocket at take off and an upright position control of a humanoid robot. Position control of Rotary Inverted Pendulum (RIP) systems (and its other variants) for the pendulum balance control problem has been widely considered and addressed in the literature (like in [35], [36], [37]). However, the balance control problem using polynomial type reference tracking has not be studied (and addressed) yet. This paper addresses the polynomial type reference position tracking problem in the context of time-varying MPC (TV-MPC).

In this article a state-space GMPC, named Time-Varying MPC (TV-MPC), formulation is presented. The algorithm starts with a direct parametrization to bring the nonlinear system to a Linear Time Varying (LTV) structure with State Dependent Coefficients (SDC). This is achieved using an efficient, novel and simple dynamics decomposition approach. The orthonormal Laguerre functions are used to approximate the feedback control trajectory which guarantees bounded Integral Square Value (ISV). A worth mentioning aspect is that the reference trajectory (a cubic polynomial type) reflects the influence of time varying position and velocity in the TV-MPC formulation. Optimality of the solutions is ensured via State-Dependent Riccati Equation (SDRE) while an exponential data weighting take care of a possible ill-conditioning of the underlying numerical structure of the TV-MPC algorithm. In addition, the modified weighting matrices, with sufficiently large prediction horizon, ensures asymptotic stability. Finally, the proposed TV-MPC algorithm is validated on a laboratory test bench system.

Rest of the paper is organized as follows. Section II provides physical and mathematical description of the subject under-actuated Quanser Inc. rotary inverted pendulum system. A dynamics decomposition method is proposed in Section III while the Time Varying Model Predictive Control (TV-MPC) is formulated in Section IV, which outlines the TV-MPC model structure, control trajectory modeling, reference trajectory generation and the proposed exponential data weighting mechanism. A comprehensive validation study of the proposed algorithm is carried out in Section V. The research has been summed up with concluding remarks in Section VI.

TABLE 1. List of acronyms.

Acronym	Description
MPC	Model predictive control
TV-MPC	Time Varying MPC
GMPC	Generalized MPC
PCD	Predictive control design
FIR	Finite impulse response
SR	Step response
DMC	Dynamic matrix control
RIP	Rotary inverted pendulum
LTV	Linear time varying
SDC	State dependent coefficients
ISV	Integral square value
SDRE	State dependent Riccati equations
EOM	Equations of motion
OCP	Optimal control problem
QP	Quadratic programming

II. THE ROTARY INVERTED PENDULUM (RIP)

The Rotary Inverted Pendulum (RIP) system, equipped with servo base unit and a pendulum rod is shown in Fig. 1 (see [38] for details).

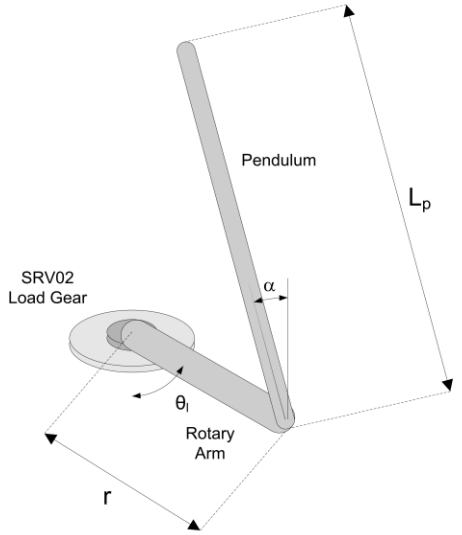

FIGURE 1. Rotary inverted pendulum conventions [38].

The nonlinear Lagrange Equations Of Motion (EOM), acquired from [38], are listed in Eq. (1).

$$\begin{aligned}\xi_1\ddot{\theta} - \xi_2\ddot{\alpha} + \xi_3\dot{\theta}\dot{\alpha} + \xi_4\dot{\alpha}^2 &= \tau - B_r\dot{\theta} \\ -\xi_2\ddot{\theta} + \xi_5\ddot{\alpha} - \xi_6\dot{\theta}^2 - \xi_7 &= -B_p\dot{\alpha} \end{aligned} \quad (1)$$

where, ξ_i, $(i = 1 - 7)$ are used for notational simplicity.

$$\begin{aligned}\xi_1 &= m_pL_r^2 + J_r + \frac{1}{4}m_pL_p^2\left(1 - \text{Cos}(\alpha)^2\right) \\ \xi_2 &= \frac{1}{2}m_pL_pL_r\text{Cos}(\alpha) \\ \xi_3 &= \frac{1}{2}m_pL_p^2\text{Sin}(\alpha)\text{Cos}(\alpha) \\ \xi_4 &= \frac{1}{2}m_pL_pL_r\text{Sin}(\alpha) \\ \xi_5 &= J_p + \frac{1}{4}m_pL_p^2 \\ \xi_6 &= \frac{1}{4}m_pL_p^2\text{Sin}(\alpha)\text{Cos}(\alpha) \\ \xi_7 &= \frac{1}{2}m_pL_pg\text{Sin}(\alpha)\end{aligned}$$

The variable τ, in Eq. (1), represent the torque generated by SRV02 servo motor and satisfies,

$$\tau = \frac{\eta_gK_g\eta_mk_t(V_m - K_gk_m\dot{\theta})}{R_m} \quad (2)$$

where, V_m is the motor input voltage. This torque is directly applied at the base of rotary arm (the load gear). A detailed description of the parameters, coined above, can be found in [38] while some of important ones are listed in Table 2.

A use of generalized coordinates, $q = [\theta \quad \alpha]^T$ and $\dot{q} = \left[\frac{d\theta}{dt} \quad \frac{d\alpha}{dt}\right]^T$, can represented Eq. (1) in Lagrangian matrix notation.

$$D(q)\ddot{q} + C(q,\dot{q})\dot{q} + g(\dot{q}) = \tau \quad (3)$$

where, $D(q)$ is the inertia matrix, $C(q,\dot{q})$ is the damping matrix and $g(\dot{q})$ is the generalized gravitational vector.

TABLE 2. Physical specifications of the quanser Inc. Inverted pendulum.

Description	Value	Unit
Mass of pendulum	0.127	kg
Total length of pendulum	0.337	m
Distance from pivot to center of mass	0.156	m
Pendulum moment of inertia	0.0012	$kg.m^2$
Mass of rotary arm	0.257	kg
Viscous damping coefficient	0.0024	$N.m.s/rad$
Rotary arm length from pivot to tip	0.216	m
Rotary arm length from pivot to center of mass	0.0619	m
Pendulum encoder resolution	4096	counts/rev

Rearranging Eq. (1), as Lagrangian matrix notation (Eq. (3)), and substitution of Eq. (2) results in the following.

$$\begin{bmatrix}\xi_1 & -\xi_2 \\ -\xi_2 & \xi_5\end{bmatrix}\begin{bmatrix}\ddot{\theta} \\ \ddot{\alpha}\end{bmatrix} + \begin{bmatrix}\xi_3\dot{\alpha} + \gamma_1 + B_r & \xi_4\dot{\alpha} \\ -\xi_6\dot{\theta} & B_p\end{bmatrix}\begin{bmatrix}\dot{\theta} \\ \dot{\alpha}\end{bmatrix} \\ \ldots + \begin{bmatrix}0 \\ -\xi_7\end{bmatrix} = \begin{bmatrix}\gamma_2 \\ 0\end{bmatrix}V_m \quad (4)$$

where, γ_i, described below, have been used for notational simplicity.

$$\begin{aligned}\gamma_1 &= \frac{\eta_gK_g^2\eta_mk_tk_m}{R_m} \\ \gamma_2 &= \frac{\eta_gK_g\eta_mk_t}{R_m}\end{aligned}$$

Solving Eq. (4) for the acceleration terms $(\ddot{\theta}, \ddot{\alpha})$ gives,

$$\begin{aligned}\ddot{\theta} &= \frac{1}{J_T}\left[\left(\xi_2\xi_6\dot{\theta} - \xi_5(\xi_3\dot{\alpha} + \gamma_1 + B_r)\right)\dot{\theta}\right]\cdots \\ &\quad - \frac{1}{J_T}\left[(\xi_4\xi_5\dot{\alpha} + \xi_2B_p)\dot{\alpha} + \xi_2\xi_7 + \xi_5\gamma_2V_m\right] \\ \ddot{\alpha} &= \frac{1}{J_T}\left[\xi_1\xi_6 - \xi_2(B_r + \gamma_1 + \xi_3\dot{\alpha})\right]\dot{\theta}\ldots \\ &\quad + \frac{1}{J_T}\left[\xi_1\xi_7 - (\xi_2\xi_4\dot{\alpha} + \xi_1B_p)\dot{\alpha} + \xi_2\gamma_2V_m\right]\end{aligned} \quad (5)$$

where, $J_T = \xi_1\xi_5 - \xi_2^2$. The state space representation reads as,

$$\begin{bmatrix}\dot{x}_1 \\ \dot{x}_2 \\ \dot{x}_3 \\ \dot{x}_4\end{bmatrix} = \begin{bmatrix}\dot{\theta} \\ \dot{\alpha} \\ f_1 \\ f_2\end{bmatrix} + \frac{1}{J_T}\begin{bmatrix}0 \\ 0 \\ \xi_5\gamma_2 \\ \xi_2\gamma_2\end{bmatrix}V_m \quad (6)$$

where,

$$\begin{aligned}f_1 &= \frac{1}{J_T}\left[\left(\xi_2\xi_6\dot{\theta} - \xi_5(\xi_3\dot{\alpha} + \gamma_1 + B_r)\right)\dot{\theta}\right]\cdots \\ &\quad - \frac{1}{J_T}\left[(\xi_4\xi_5\dot{\alpha} + \xi_2B_p)\dot{\alpha} + \xi_2\xi_7\right] \\ f_2 &= \frac{1}{J_T}\left[\xi_1\xi_6 - \xi_2(B_r + \gamma_1 + \xi_3\dot{\alpha})\right]\dot{\theta}\ldots \\ &\quad + \frac{1}{J_T}\left[\xi_1\xi_7 - (\xi_2\xi_4\dot{\alpha} + \xi_1B_p)\dot{\alpha}\right]\end{aligned}$$

Then, Eq. (6) is in generic and standard (normal) form.

$$\dot{x}(t) = f(x) + g(x)u \tag{7}$$

Here, $f(x) = A(x)x$ is the proposed dynamic decomposition. Now the goal is to compute the *decomposition* $A(x)$.

III. THE DYNAMICS DECOMPOSITION APPROACH

A simplest procedure to compute $A(x)$ is presented here. The idea is based on the following decomposition described for a scalar function $f(x)$ of three variables $x = [x_1\ x_2\ x_3]^T$.

$$\begin{aligned} f(x_1, x_2, x_3) = &\left(\frac{f(x_1, x_2, x_3) - f(0, x_2, x_3)}{x_1}\right) x_1 \cdots \\ &+ \left(\frac{f(0, x_2, x_3) - f(0, 0, x_3)}{x_2}\right) x_2 \cdots \\ &+ \left(\frac{f(0, 0, x_3) - f(0, 0, 0)}{x_3}\right) x_3 \end{aligned} \tag{8}$$

The equation above is a way of expressing a function of three variables, $f(x_1, x_2, x_3)$, as a sum of three terms, each involving only one variable. This is called a *Taylor expansion* of the function around the origin $(0, 0, 0)$. It is useful for approximating the value of the function near the origin, when the variables are small. The equation can be derived by applying the *chain rule* of differentiation to the function and evaluating the partial derivatives at the origin. The equation can be interpreted as follows: the value of the function at any point (x_1, x_2, x_3) is approximately equal to the value of the function at the origin, plus the change in the function due to moving along the x_1 axis, plus the change in the function due to moving along the x_2 axis, plus the change in the function due to moving along the x_3 axis. The decomposition in Eq. (8) is dependent on the order of the variables and must certainly solve the division by zero.

A procedure for computation of the decomposition $A(x)$ is shown in Fig. 2 for an arbitrary state vector x and numerical accuracy *eps* of the computer. This algorithm compute $A(x)$ for each value of x while taking care of the *division by zero* problem. However, the computation of this decomposition is not unique. The above coined approach is utilized to *decompose* the nonlinear dynamics, $f(x_m) = A_m(x_m)x_m$ in Eq. (6), with an order of variables (choice of state vector) $x_m = [\theta\ \alpha\ \dot{\theta}\ \dot{\alpha}]^T$.

$$\begin{aligned} f(\theta, \alpha, \dot{\theta}, \dot{\alpha}) = &\frac{f(\theta, \alpha, \dot{\theta}, \dot{\alpha}) - f(0, \alpha, \dot{\theta}, \dot{\alpha})}{\theta}\theta \\ &+ \ldots \frac{f(0, \alpha, \dot{\theta}, \dot{\alpha}) - f(0, 0, \dot{\theta}, \dot{\alpha})}{\alpha}\alpha \\ &+ \ldots \frac{f(0, 0, \dot{\theta}, \dot{\alpha}) - f(0, 0, 0, \dot{\alpha})}{\dot{\theta}}\dot{\theta} \\ &+ \ldots \frac{f(0, 0, 0, \dot{\alpha}) - f(0, 0, 0, 0)}{\dot{\alpha}}\dot{\alpha} \\ = &\, A_m(x_m)x_m \end{aligned} \tag{9}$$

With,

$$A_m(x_m) = \begin{bmatrix} \frac{f(\theta, \alpha, \dot{\theta}, \dot{\alpha}) - f(0, \alpha, \dot{\theta}, \dot{\alpha})}{\theta} \\ \frac{f(0, \alpha, \dot{\theta}, \dot{\alpha}) - f(0, 0, \dot{\theta}, \dot{\alpha})}{\alpha} \\ \frac{f(0, 0, \dot{\theta}, \dot{\alpha}) - f(0, 0, 0, \dot{\alpha})}{\dot{\theta}} \\ \frac{f(0, 0, 0, \dot{\alpha}) - f(0, 0, 0, 0)}{\dot{\alpha}} \end{bmatrix}^T,$$

$$B_m(x_m) = g(x_m) = \frac{1}{J_T}\begin{bmatrix} 0 \\ 0 \\ \xi_5\gamma_2 \\ \xi_2\gamma_2 \end{bmatrix},$$

$$C_m = \begin{bmatrix} 1 & 0 & 0 & 0 \\ 0 & 1 & 0 & 0 \\ 0 & 0 & 1 & 0 \\ 0 & 0 & 0 & 1 \end{bmatrix},$$

$$D_m = 0 \tag{10}$$

and,

$$\begin{aligned} &\frac{f(\theta, \alpha, \dot{\theta}, \dot{\alpha}) - f(0, \alpha, \dot{\theta}, \dot{\alpha})}{\theta} \\ &= \begin{bmatrix} 0 \\ 0 \\ 0 \\ 0 \end{bmatrix}, \\ &\frac{f(0, \alpha, \dot{\theta}, \dot{\alpha}) - f(0, 0, \dot{\theta}, \dot{\alpha})}{\alpha} \\ &= \frac{1}{\alpha}\begin{bmatrix} 0 \\ 0 \\ \frac{\xi_8\xi_9 + J_T\xi_{10}}{\xi_{11}} \\ \frac{\xi_8\xi_{12} + J_T\xi_{13}}{\xi_{11}} \end{bmatrix}, \\ &\frac{f(0, 0, \dot{\theta}, \dot{\alpha}) - f(0, 0, 0, \dot{\alpha})}{\dot{\theta}} \\ &= \begin{bmatrix} 1 \\ 0 \\ \frac{(\gamma_1 + B_r)}{(m_pL_r^2 + J_r)} \\ -\frac{\left(\frac{1}{2}m_pL_pL_r\right)(\gamma_1 + B_r)}{(m_pL_r^2 + J_r)\left(J_p + \frac{1}{4}m_pL_p^2\right)} \end{bmatrix}, \\ &\frac{f(0, 0, 0, \dot{\alpha}) - f(0, 0, 0, 0)}{\dot{\alpha}} \end{aligned}$$

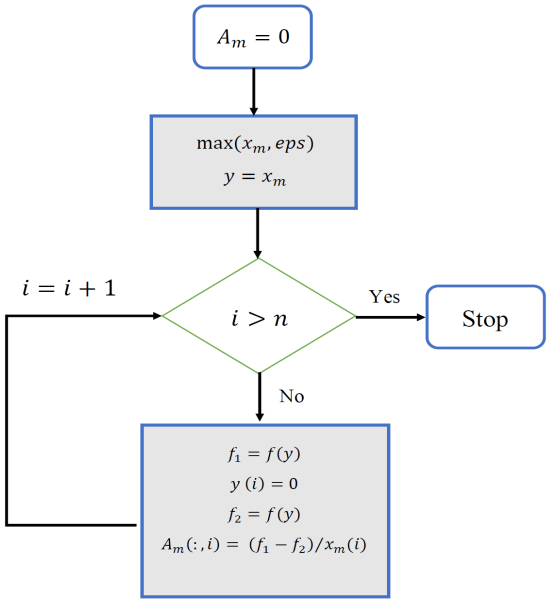

FIGURE 2. Computation of decomposition.

$$= \begin{bmatrix} 0 \\ 1 \\ -\dfrac{\left(\frac{1}{2}m_p L_p L_r\right) B_p}{\left(m_p L_r^2 + J_r\right)\left(J_p + \frac{1}{4}m_p L_p^2\right)} \\ \dfrac{-B_p}{\left(J_p + \frac{1}{4}m_p L_p^2\right)} \end{bmatrix} \tag{11}$$

where,

$$\begin{aligned}
\xi_8 &= \left(m_p L_r^2 + J_r\right)\left(J_p + \frac{1}{4}m_p L_p^2\right), \\
\xi_9 &= \left(\xi_2\xi_6\dot{\theta} - \xi_5(\xi_3\dot{\alpha} + \gamma_1 + B_r)\right)\dot{\theta} \cdots \\
&\quad - \left(\xi_4\xi_5\dot{\alpha} + \xi_2 B_p\right)\dot{\alpha} + \xi_2\xi_7, \\
\xi_{10} &= \left(J_p + \frac{1}{4}m_p L_p^2\right)(\gamma_1 + B_r)\,\dot{\theta} + \cdots \\
&\quad + \left(\frac{1}{2}m_p L_p L_r\right) B_p\dot{\alpha}, \\
\xi_{11} &= J_T\left(m_p L_r^2 + J_r\right)\left(J_p + \frac{1}{4}m_p L_p^2\right), \\
\xi_{12} &= \left(\xi_1\xi_6\dot{\theta} - \xi_2(\xi_3\dot{\alpha} + \gamma_1 + B_r)\right)\dot{\theta} \cdots \\
&\quad - \left(\xi_2\xi_4\dot{\alpha} + \xi_1 B_p\right)\dot{\alpha} + \xi_1\xi_7, \\
\xi_{13} &= \left(\frac{1}{2}m_p L_p L_r\right)(\gamma_1 + B_r) \cdots \\
&\quad + \left(m_p L_r^2 + J_r\right) B_p\dot{\alpha}
\end{aligned} \tag{12}$$

This dynamic decomposition providing matrix pair $(A_m(x_m), B_m(x_m))$, is extremely useful, efficient and simple. It enables assessment of controllability of the said rotary inverted pendulum analogous to that of an LTI-system.

For the proposed TV-MPC design, following assumptions are valid:

Assumption 3.1: The entire time varying behavior is divided into N_s discrete time instants t_i with an associated LTI model (a total of N_s models). Each LTI model reflects the time varying behavior in piece-wise fashion. Thus, the entire time variation is covered from initial time t_0 to the final time t_f.

Assumption 3.2: All the states are measurable.

Assumption 3.3: The pair $(A(x_m(t_i)), B(x_m(t_i)))$ is completely controllable and the pair $(A(x_m(t_i)), C)$ is completely observable.

IV. TIME-VARYING MODEL PREDICTIVE CONTROL FORMULATION

Inspired from the proposal in [30], a continuous-time MPC paradigm is presented. The proposed MPC, termed as Time-Varying MPC (TV-MPC), handles state dependent time-varying model structures in the state space (obtained via novel dynamic decomposition). Moreover, the proposed TV-MPC is based on the receding horizon principle for future control trajectory modeling.

A distinction, to use the continuous time formalism, is to tackle the problem of irregular sampling. Since, the TV-MPC formulation is based on the continuous-time dynamically decomposed models (independent of the sampling interval in the formulation). Thus, it permits irregular sampling and provides more robustness, flexibility, computational efficiency and better performance for fast sampling rates. Though, the actual implementation is done in discrete-time on actual computer (or embedded hardware).

A. TV-MPC MODEL STRUCTURE

The proposed TV-MPC model structure is equipped with a built-in integrator (considering $\dot{u}(t)$ as the control input). To start with, an augmented state space model of rotary inverted pendulum system is presented in Eq. (13).

$$\begin{aligned}
\dot{x}(t_i) &= \begin{bmatrix} \dot{z}(t_i) \\ \dot{e}(t_i) \end{bmatrix} = \overbrace{\begin{bmatrix} A_m(x_m(t_i)) & 0_m \\ C_m & 0_{q\times q} \end{bmatrix}}^{A(x_m(t_i))} \begin{bmatrix} z(t_i) \\ e(t_i) \end{bmatrix} \cdots \\
&\quad + \overbrace{\begin{bmatrix} B_m(x_m(t_i)) \\ 0_{q\times m} \end{bmatrix}}^{B(x_m(t_i))} \dot{u}(t_i) \\
y(t_i) &= \underbrace{\begin{bmatrix} 0_m & I_{q\times q} \end{bmatrix}}_{C} \begin{bmatrix} z(t_i) \\ e(t_i) \end{bmatrix}
\end{aligned} \tag{13}$$

where, $q = 2$, $m = 1$, $i = 0, 1, \ldots N_s$, $e(t_i) = y(t_i) - r(t_i)$, $z(t_i) = \dot{x}_m(t_i) = \left[\dot{\theta}(t_i)\ \dot{\alpha}(t_i)\ \ddot{\theta}(t_i)\ \ddot{\alpha}(t_i)\right]^T$, $r(t_i) = \left[\theta_{ref}(t_i)\ \dot{\theta}_{ref}(t_i)\right]^T$, $y(t_i) = C_m x_m(t_i)$. The augmented time varying, state-dependent model triplets are $(A(x_m(t_i)), B(x_m(t_i)), C)$. Then, Eq. (13) can also be written in the form,

$$\begin{aligned}
\dot{x}(t_i) &= A(x_m(t_i))x(t_i) + B(x_m(t_i))\dot{u}(t_i) \\
y(t_i) &= Cx(t_i)
\end{aligned} \tag{14}$$

Moreover, the total number of samples N_s, from t_0 to t_f, with a sampling interval h, is simply given by $N_s = \frac{t_f - t_0}{h}$. As can be seen from Eq. (13) that $y(t_i) = e(t_i)$ which is the prediction error thus taking into account the on-line error measurements from the measured states.

B. CONTROL TRAJECTORY MODELING: RECEDING HORIZON CONTROL

The control trajectory $\dot{u}(t)$ modeling, using the matrix pairs $(A(x_m(t_i)), B(x_m(t_i)))$ and $(A(x_m(t_i)), C)$, in conjunction with Laguerre functions, is described here. The future control trajectory $\dot{u}(t)$ is modelled using Laguerre functions and is presented in Eq. (15) by considering a moving time window from t_i to $t_i + T_p$, with $0 \leq t_i \leq T_p$ and $T_p \geq 0$, as the prediction horizon.

$$\dot{u}(t_i) \approx \sum_{i=1}^{N_l} c_i l_i(\tau) = L^T(t_i)\eta \tag{15}$$

where, η is the coefficient vector and N_l is the number of Laguerre terms (simply, the order of Laguerre filter). The term, $L(t_i) = \left[l_1(t_i)\ l_2(t_i) \cdots l_{N_l}(t_i)\right]^T$, is a set of pre-chosen Laguerre functions satisfying the following equation with p denoting the scaling factor for Laguerre functions and initial conditions $L(0) = \sqrt{2p}\,[1\ 1\ \ldots\ 1]^T$.

$$\dot{L}(t_i) = \underbrace{\begin{bmatrix} -p & 0 & \ldots & 0 \\ -2p & -p & \ldots & 0 \\ \vdots & \vdots & \vdots & \vdots \\ -2p & \ldots & -2p & -p \end{bmatrix}}_{A_p} L(t_i) \tag{16}$$

Assuming that the state variable $x(t_i)$, at current time t_i, is available, then at any future time $\tau > 0$ the predicted future state, $x(t_i + \tau|t_i)$, is given by the following equation.

$$\begin{aligned} x(t_i + \tau|t_i) &= e^{A(x_m(t_i))\tau} x(t_i) \\ &\quad + \cdots \int_0^{\tau} e^{A(x_m(t_i))(\tau - \vartheta)} B(x_m(t_i)) \dot{u}(\vartheta) d\vartheta \end{aligned} \tag{17}$$

Here, ϑ is the variable of integration. Accordingly, the plant output prediction is represented by,

$$y(t_i + \tau|t_i) = Cx(t_i + \tau|t_i) \tag{18}$$

In Eq. (17) the solution of convolutional integral is found via algebraic matrix equation (see [27], [28]).

The TV-MPC is always subjected to an optimization routine. This is done with a cost function coined in Eq. (19) with set point $r(t_i)$. In addition to optimum control input, it allows specifying the performance metrics by selecting weights $Q \geq 0$ and $R \geq 0$.

$$\begin{aligned} \mathcal{J} &= \int_0^{T_p} \left(\dot{u}^T(\tau) R \dot{u}(\tau)\right) d\tau \\ &\quad + \cdots \int_0^{T_p} \left([r(t_i) - y(t_i + \tau|t_i)]^T\, Q\, [r(t_i) - y(t_i + \tau|t_i)]\right) d\tau \end{aligned} \tag{19}$$

Without constraints, the aim of proposed TV-MPC treatment is to find a control law such that the predicted plant outputs $\theta(t_i + \tau|t_i)$ and $\dot{\theta}(t_i + \tau|t_i)$ tracks the future trajectory of the set-point $r(t_i)$ as close as possible in least square sense.

Since, $C = [0\ \ I_{2\times 2}]$ and choosing $Q = C^T C$ in conjunction with the augmented model, the cost function gets the form,

$$\begin{aligned} \mathcal{J} &= \int_0^{T_p} \left(\dot{u}^T(\tau) R \dot{u}(\tau)\right) d\tau \\ &\quad + \cdots \int_0^{T_p} \left(x^T(t_i + \tau|t_i) Q x(t_i + \tau|t_i)\right) d\tau \end{aligned} \tag{20}$$

where, the initial state variable information $x(t_i)$ contains the error $y(t_i) - r(t_i)$ instead of $y(t_i)$. After substituting $x(t_i + \tau|t_i)$ into Eq. (20) and using the orthonormal property of Laguerre functions for the term $\int_0^{T_p} \dot{u}^T(\tau) R \dot{u}(\tau) d\tau$, the cost function in terms of η is,

$$\begin{aligned} \mathcal{J} &= \int_0^{T_p} \left(\eta^T R_L \eta\right) d\tau \\ &\quad + \cdots \int_0^{T_p} \left(x^T(t_i + \tau|t_i) Q x(t_i + \tau|t_i)\right) d\tau \\ &= \eta^T \Omega \eta + 2\eta^T \psi x(t_i) \cdots \\ &\quad + x^T(t_i) \int_0^{T_p} e^{A(x_m(t_i))\tau} d\tau\, x(t_i) \end{aligned} \tag{21}$$

where,

$$\begin{aligned} \Omega &= R_L + \int_0^{T_p} \phi(\tau) Q \phi^T(\tau) d\tau \\ \psi &= \int_0^{T_p} \phi(\tau) Q e^{A(x_m(t_i))\tau} d\tau \end{aligned} \tag{22}$$

The optimal η that minimizes $\mathcal{J}$ (without hard constraints) is,

$$\eta = -\Omega^{-1} \psi x(t_i) \tag{23}$$

and the minimum of the cost function is,

$$\begin{aligned} \mathcal{J}_{min} &= x^T(t_i) \left[\int_0^{T_p} \left(e^{A(x_m(t_i))\tau} Q e^{A(x_m(t_i))\tau}\right) d\tau\right] x(t_i) \\ &\quad - x^T(t_i) \left[\int_0^{T_p} \left(\psi^T \Omega^{-1} \psi\right) d\tau\right] x(t_i) \end{aligned} \tag{24}$$

In Eq. (21), R_L is a block diagonal matrix with the k-th block $(k = 0, 1, 2, \ldots, m)$ being $R_k = r_k I_{N_s^k \times N_s^k}$. In the presented study, $m = 1$ and $I_{N_s^k \times N_s^k}$ is a unit matrix. The optimal control, trajectory for the unconstrained problem with finite prediction horizon at time t_i is,

$$\dot{u}(t_i) = \begin{bmatrix} L_1^T(0) & 0_2 & \cdots & 0_m \\ 0_1 & L_2^T(0) & \cdots & 0_m \\ \vdots & \vdots & \vdots & \vdots \\ 0_1 & 0_2 & \cdots & L_m^T(0) \end{bmatrix} \begin{bmatrix} \eta_1 \\ \eta_2 \\ \vdots \\ \eta_m \end{bmatrix} \tag{25}$$

Since the rotary inverted pendulum system has only one input ($m = 1$) which is applied directly to the rotary servo motor arm and the only state directly actuated is $\theta(t)$. Thus, Eq. (25) is reduced to the following form.

$$\dot{u}(t_i) = L_1^T(0)\eta_1 \tag{26}$$

Substitution of $\eta_1 = \eta$, from Eq. (23), in Eq. (26), the final expression for the optimal TV-MPC controller is obtained as follows.

$$\dot{u}(t_i) = -\underbrace{L_1^T(0)\Omega^{-1}\psi}_{K_{mpc}(x_m(t_i))} x_m(t_i) \tag{27}$$

where, $K_{mpc}(.)$ is the feedback TV-MPC gain matrix. When hard constraints are enforced in the design, then the continuous time TV-MPC problem becomes the minimization of the cost function in Eq. (21) subject to the linear inequality constraints of the form,

$$M\eta \leq \Upsilon \tag{28}$$

The procedure to formulate these inequality constraints in continuous time MPC designs is mentioned in details in [32] and [33]. As with other MPC algorithms, the Quadratic Programming (QP) methods can be deployed to find the unique constrained solution, if following conditions are satisfied in context,

- The invertability of Hessian matrix Ω.
- The linear independence of active constraints at time t_i
- The dimensions of η to be greater than the number of active constraints.

For details on constrained MPC formulation in continuous time domain and application of QP methods for such problems, reader is referred to [28], [39], [40], and [32].

The receding horizon control demands using the derivative of future control action at $\tau = 0$. However, in digital implementation an Euler approximation is usually used for $\dot{u}(t_i)$.

$$\begin{aligned} \dot{u}(t_i) &= \frac{u(t_i) - u(t_i - h)}{h} \\ u(t_i) &= u(t_i - h) + \dot{u}(t_i)h \end{aligned} \tag{29}$$

While the actual control, using Eq. (29), is written as,

$$u_{act}(t_i) = u_{ss} + u(t_i) \tag{30}$$

where, $u_{act}(t_i)$ and u_{ss} are the actual and steady state controls at t_i respectively while h is the sampling interval. Further mathematical manipulations give the following expression.

$$\begin{aligned} u_{act}(t_i - h) &= u_{ss} + u(t_i - h) \\ u_{act}(t_i) &= u_{act}(t_i - h) + \dot{u}(t_i)h \\ u_{act}(t_i) &= u_{act}(t_i - h) + L_1^T(0)\eta_1 h \end{aligned} \tag{31}$$

where, $u_{act}(t_i - h)$ is the control signal at previous sampling instant and $u_{act}(t_i)$ is the actual control to the rotary inverted pendulum system.

The implementation of control in the form of Eq. (31) is advantageous in applications specifically involving a position tracking (as the present study implies), since the actual control does not depend on the steady state value. Instead, the actual control will repeatedly update itself from its past values.

C. NUMERICAL CONDITIONING AND EXPONENTIAL DATA WEIGHTING

The ill conditioning of Hessian matrix, caused by increasing prediction horizon, is highlighted and an exponential data weighting [27], [41], [42] approach is incorporated to handle this issue.

The core reason behind ill conditioning is unstable model in the design structure used for prediction. The unstable prediction emerges from the unstable matrix $A(x_m(t_i))$ resulting after the addition of embedded integrator in the model for integral action.

A remedy is to scale $A(x_m(t_i))$, using exponential data weighting, such that resulting scaled matrix $A_\gamma(x_m(t_i))$ is strictly Hurwitz (with eigenvalues *strictly* in the Left-Half-Plane (LHP)). This scaling essentially transforms the original state and derivative of the control variables into exponentially weighted variables for optimization procedure. This is also an important aspect of Laguerre functions as well, that with stable prediction model, these functions can model the future control trajectory very well and much precisely with guaranteed convergence [27]. Therefore the L_2 stability condition of Laguerre functions is satisfied by using Hurwitz matrix $A_\gamma(x_m(t_i))$ in the design.

The introduction of function $e^{-2\gamma\tau}$, with $\gamma > 0$, effectively produces an exponentially decreasing weight and the Optimal Control Problem (OCP) modifies to the following form,

$$\begin{aligned} \min_{\dot{u}(\tau)} \mathcal{J} = &\int_0^{T_p} x_\gamma^T(t_i + \tau|t_i) Q x_\gamma(t_i + \tau|t_i) d\tau \\ &+ \int_0^{T_p} \dot{u}_\gamma^T(\tau) R \dot{u}_\gamma(\tau) d\tau \end{aligned} \tag{32}$$

$$\begin{aligned} \text{subjected to, } \dot{x}_\gamma(t_i + \tau|t_i) = &[A(x_m(t_i)) - \gamma I]\, x_\gamma(t_i + \tau|t_i) \\ &+ B(x_m(t_i))\dot{u}_\gamma(t_i) \end{aligned} \tag{33}$$

where, the transformed variables are defined by,

$$\begin{aligned} x_\gamma(t_i + \tau|t_i) &= e^{-\gamma\tau} x(t_i + \tau|t_i) \\ \dot{u}_\gamma(\tau) &= e^{-\gamma\tau}\dot{u}(\tau) \end{aligned} \tag{34}$$

The initial conditions are identical for $\tau = 0$ and the scaling matrix $A_\gamma(x_m(t_i)) = A(x_m(t_i)) - \gamma I$ is Hurwitz. Thus, eradicating the hazard of numerical ill-conditioning.

The exponential decay of $x(t_i + \tau|t_i)$ is not guaranteed with Q and R in the optimization window. To cope with, a slight modification is made to the weight matrix Q (see [27], [28], [42]) such that $Q_\gamma = Q + 2\gamma P$ with $\gamma > 0$. The optimal control $\dot{u}(\tau)$ is then followed from minimizing the OCP in Eq. (32) and (33), with Q_γ in the cost function. Moreover, the time-varying matrix P, in Q_γ, is the solution of a steady

state SDRE.

$$A^T(x_m(t_i))P + PA(x_m(t_i)) \cdots - PB(x_m(t_i))R^{-1}B^T(x_m(t_i))P + Q = 0 \quad (35)$$

The proposed setup eradicates the deviation of optimal solution from the original one even if T_p is sufficiently large.

Furthermore, a prescribed degree of stability is introduced, in the predictive control, such that all closed loop Eigen values are on the left of line $s = -\beta$. This is achieved via a further modification to the matrix Q_γ.

$$Q_\gamma = Q + 2(\gamma + \beta)P \quad (36)$$

The time-varying matrix P is now the solution to a modified steady state SDRE.

$$A_\gamma^T(x_m(t_i))P + PA_\gamma(x_m(t_i)) \cdots - PB(x_m(t_i))R^{-1}B^T(x_m(t_i))P + Q_\gamma = 0 \quad (37)$$

where, $A_\gamma(x_m(t_i)) = A(x_m(t_i)) - \gamma I$. It is worth mentioning that the terms T_p, p, N_l, γ, β, Q and R are the tuning parameters and are set as per design specifications and requirements.

D. REFERENCE TRAJECTORY GENERATION

In the proposed TV-MPC treatment, of a rotary inverted pendulum, a reference trajectory of cubic polynomial type is chosen which is smooth and piece-wise continuous. The reference trajectories for position and velocity are originated right away from the ramp (reference acceleration) profiles for the initial and final values of position and velocity respectively. Therefore, cubic polynomial type reference trajectories reflect the time varying position and velocity dynamics much better into the time-varying, state dependent model structure and henceforth in the entire problem as well. Maintaining the continuity of derivatives ensures smooth motions and can be used to generate trajectories that do not require step inputs to the actuators. Polynomial type trajectories also allow for the analytical solution via elimination as constrained Quadratic Programming (QP).

Let $\theta_{ref}(t_0)$ and $\dot{\theta}_{ref}(t_0)$ are position and velocity of the rotary servo arm, respectively at initial time t_0 and $\theta_{ref}(t_f)$ and $\dot{\theta}_{ref}(t_f)$ be the position and velocity counterparts at final time t_f, then the initial and final values of rotary servo arm's acceleration are $w_\theta(t_0)$ and $w_\theta(t_f)$, respectively and are computed as,

$$\begin{bmatrix} w_\theta(t_0) \\ w_\theta(t_f) \end{bmatrix} = \begin{bmatrix} t_f - \frac{t_f}{2} & \frac{t_f}{2} \\ \frac{t_f^2}{2} - \frac{t_f^2}{6} & \frac{t_f^2}{6} \end{bmatrix}^{-1} \begin{bmatrix} \dot{\theta}_{ref}(t_f) - \dot{\theta}_{ref}(t_0) \\ \theta_{ref}(t_f) - \theta_{ref}(t_0).. \\ -\dot{\theta}_{ref}(t_0)t_f \end{bmatrix} \quad (38)$$

A mathematical manipulation, with cubic polynomials, result in the following respective expressions for reference position and velocity profiles of the rotary servo motor.

$$\theta_{ref}(t) = \theta_{ref}(t_0) + \dot{\theta}_{ref}(t_0)t + \frac{w_\theta(t_0)}{2}t^2 + \frac{\Delta_w}{6t_f}t^3$$
$$\dot{\theta}_{ref}(t) = \dot{\theta}_{ref}(t_0) + w_\theta(t_0)t + \frac{\Delta_w}{2t_f}t^2 \quad (39)$$

where, $\Delta_w = w_\theta(t_f) - w_\theta(t_0)$. The proposed continuous-time TV-MPC design work-flow is illustrated graphically in Fig. 3.

V. RESULTS AND DISCUSSION

A demonstration of the efficiency, robustness, accuracy, performance and issues like numerical stability and conditioning, of the proposed TV-MPC, is contrasted with a case study under-actuated Quanser's rotary inverted pendulum system. The study is carried out in two sub cases. In *Case-A*, the TV-MPC results, without exponential data weighting, are discussed while in *Case-B*, the merits after the deployment of exponential data weighting are discussed. Moreover, The nonlinear equations of motion and the associated parameters are adapted from [38].

A. CASE-A: NO EXPONENTIAL DATA WEIGHTING-

The influence of unstable $A(x_m(t))$ and the effect of large prediction horizon T_p on the numerical conditioning of the overall TV-MPC, without exponential data weighting, is discussed. The parameters for the simulation are tabulated in Table 3. The predicted and measured states for the pendulum rod angle ($\alpha_{pred}(t)$ and $\alpha_m(t)$, respectively) and position ($\theta_{pred}(t)$ and $\theta_m(t)$, respectively) are shown in Fig. 4 while the respective velocities ($\dot{\alpha}_{pred}(t)$, $\dot{\alpha}_m(t)$, $\dot{\theta}_{pred}(t)$ and $\dot{\theta}_m(t)$) are highlighted in Fig. 5. It may be observed that the proposed TV-MPC provide a perfect prediction of the system's states. As a result it can be seen from Figs. 6 that the servo motor arm's position efficiently track the cubic polynomial references ($\theta_{ref}(t)$ and $\dot{\theta}_{ref}(t)$) between $\pm 20^0$ (± 0.3481 [rad]) with slight (almost negligible) position error. Moreover, it may be observed that the initial and final boundary conditions are met with the prediction error evolving with a negligible magnitude of 0.046 [rad] for $\theta(t)$. Such tracking of the reference trajectory cause the pendulum rod to perfectly balance such that $\alpha_m(t) \rightarrow \varepsilon$ (with ε being a very small number and $\varepsilon \neq 0$). The predicted and measured velocity profiles for the rotary servo arm tracks the defined parabolic velocity reference (resulting from cubic interpolation) perfectly with negligible error (see Fig. 5). Though we are more interested in the position errors actually. The measured and predicted velocities results for the pendulum rod shows somewhat the physical and actual insight of the velocity profile variation as the servo arm position varies in timely fashion, as shown in Fig. 5.

The measured and predicted control trajectories ($V(t)$), along with their counterpart derivatives, are shown in Fig. 7. It is worth mentioning that the derivative of the measured control input ($\dot{V}_m(t)$) has been computed from the measured states $\theta_m(t)$, $\dot{\theta}_m(t)$, $\alpha_m(t)$ and $\dot{\alpha}_m(t)$, based on actual and

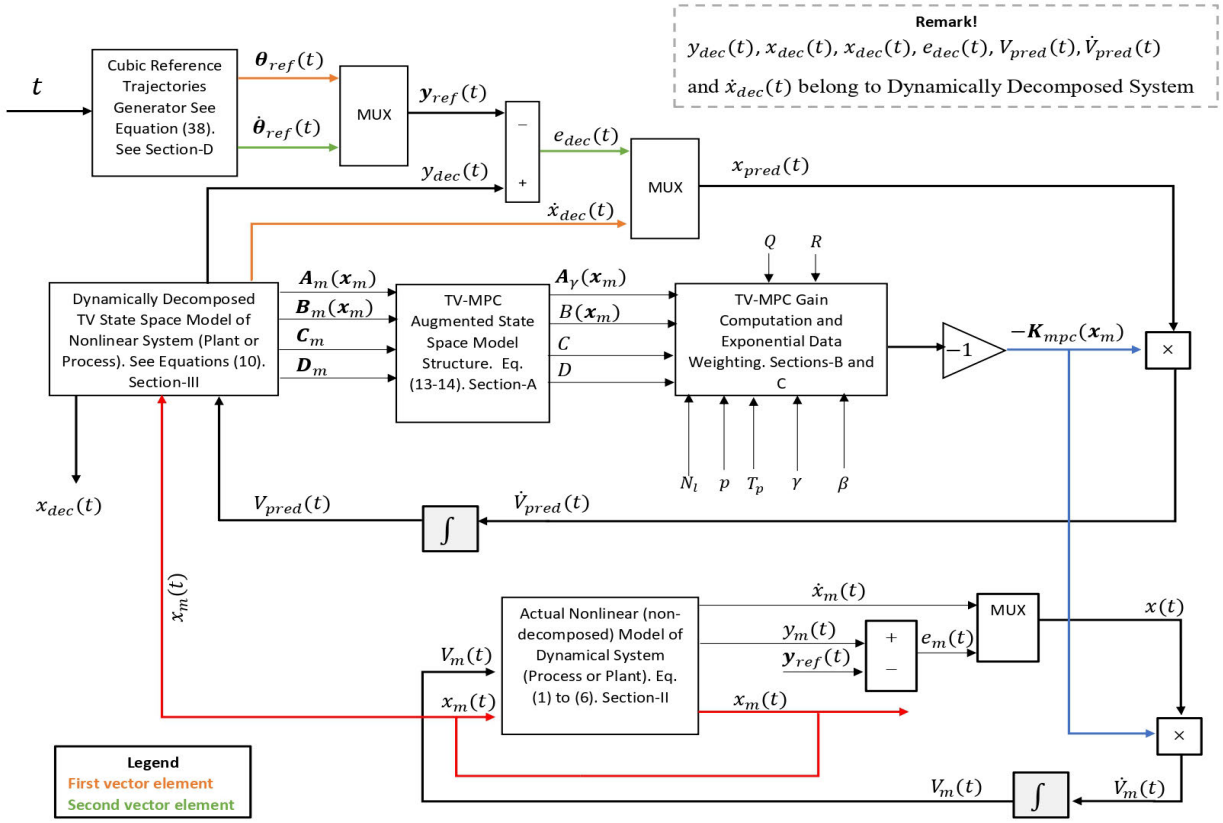

FIGURE 3. Block diagram of the proposed continuous-time TV-MPC with dynamics decomposition.

TABLE 3. *Case A* simulation specifications.

Parameter	Value
T_p	2 sec
Q	$800 \times C^T C$
R	0.01
p	1.1
N_l	50
$\theta_{ref}(t_0)$	$-20^0 = -0.3491$ rad
$\theta_{ref}(t_f)$	$20^0 = 0.3491$ rad
t_0	0 sec
t_f	10 sec
h	0.01 sec

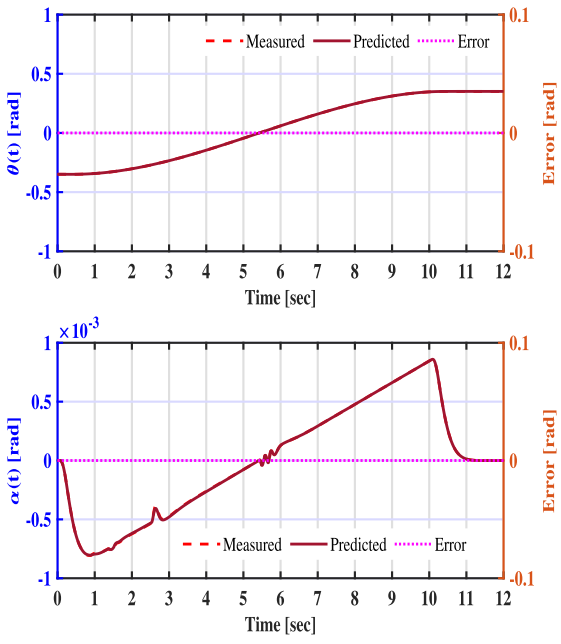

FIGURE 4. Measured versus predicted trajectories for $\theta(t)$ and $\alpha(t)$ without exponential data weighting.

non-decomposed plant's dynamics. It may be noticed that both $\dot{V}_m(t)$ and $\dot{V}_{pred}(t)$ perfectly overlap. As mentioned earlier, $\dot{V}_{pred}(t)$ is the modeled trajectory, serving as the input to the augmented state space model resulting from the dynamically decomposed model. Since, $\dot{V}_m(t)$ and $\dot{V}_{pred}(t)$ perfectly overlap each other thus an integration of either gives the actual control $V(t)$ which is applied to the Quanser Inc. rotary inverted pendulum system.

A confirmation of the efficacy (in terms of reflecting the nonlinear (time varying) dynamical behavior of the system) of the proposed dynamic decomposition is carried out via fitness assessment of the dynamically decomposed model to that of the actual (non-decomposed) nonlinear model of the

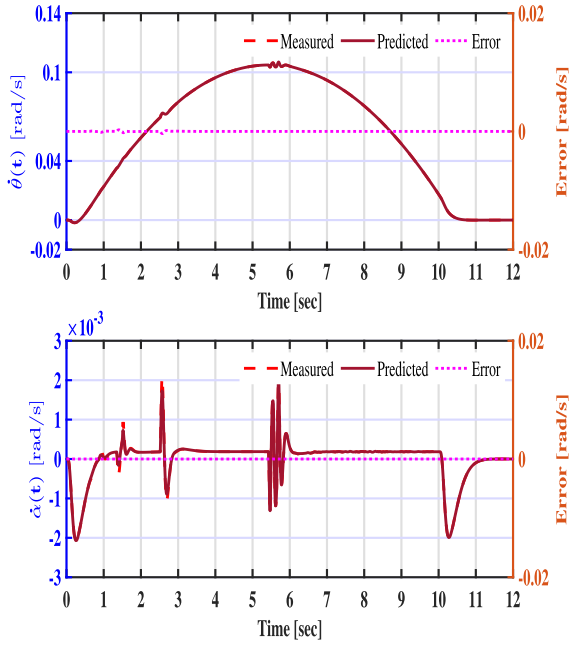

FIGURE 5. Measured versus predicted trajectories for $\dot{\theta}(t)$ and $\dot{\alpha}(t)$ with no exponential data weighting.

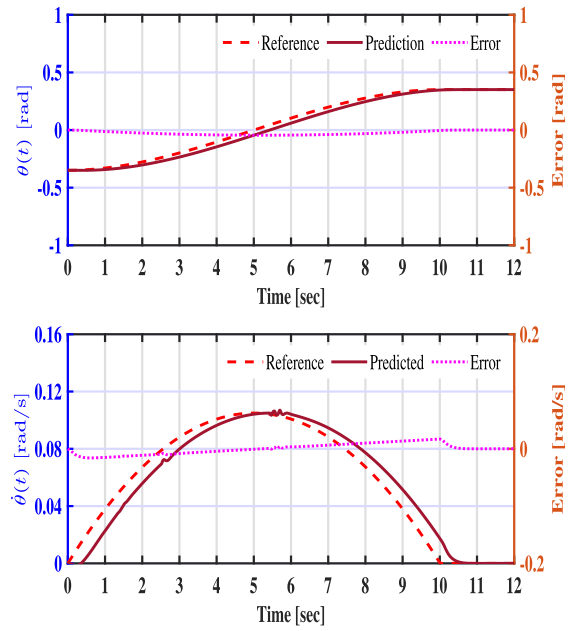

FIGURE 6. Reference versus predicted/measured trajectories for position $\theta_{pred}(t)$ and $\dot{\theta}_{pred}(t)$ without exponential data weighting.

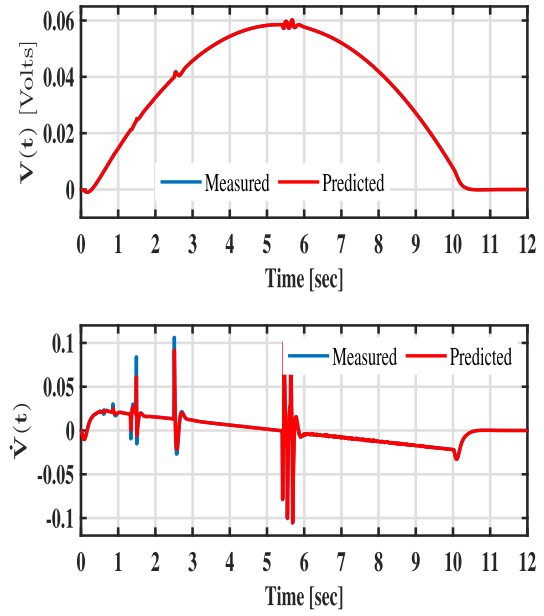

FIGURE 7. Control trajectories $V(t)$ and $\dot{V}(t)$ without exponential data weighting.

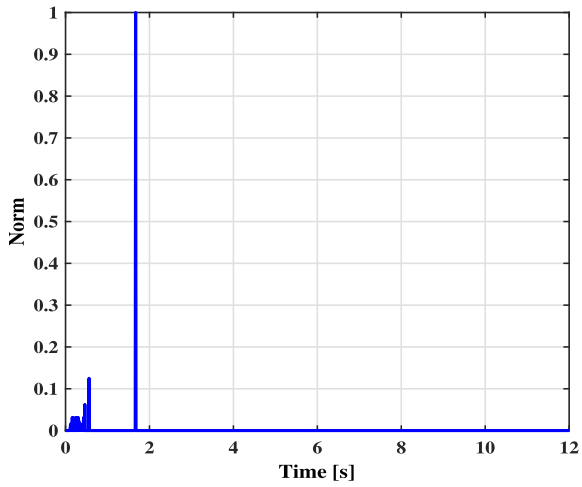

FIGURE 8. Fitness assessment for actual and prediction models without exponential data weighting.

Quanser Inc. rotary inverted pendulum system. The result is shown in Fig. 8. This fitness has been inspected for the Euclidean norm minimization of system matrices $A_{pred}(x_{pred})$ and $A_m(x_m)$ such that $\| A_{pred}(x_{pred}) - A_m(x_m) \|_2 < \delta$. Here δ is some small number confirming the boundness. The fitness plot in Fig. 8 shows that both the dynamically decomposed model and the actual nonlinear model fits well and are almost identical. The slight deterioration between $0 - 2\,sec$ (effect can be seen in previous plots in this section) are bounded and can safely be considered negligible. This is the main feature and advantage of the proposed TV-MPC paradigm.

Despite adhering to the aim of perfect reference position tracking for cubic polynomial type trajectories, the TV-MPC algorithm in *case-A* does not provide a well-conditioned numerical treatment, as the condition number $\kappa(\Omega)$ for Hessian matrix Ω is 2.82×10^{13}. This of course is too high and a slight modification in any parameter within the TV-MPC would cause the entire algorithm numerically unstable and thus Hessian matrix Ω may become non-invertible (singular). The effect of ill-conditioning is also obvious from the result of Fig. 7 where the spikes in $\dot{V}_{pred}(t)$ and $\dot{V}_m(t)$ show that further increase in the prediction horizon or change in any of the parameter within the algorithm will deteriorate the

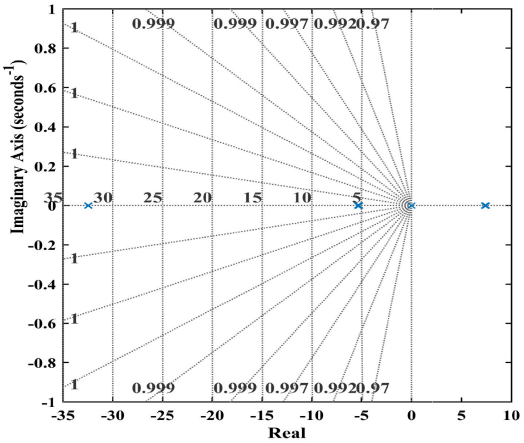

FIGURE 9. Pole-zero map for stability assessment without exponential data weighting.

TABLE 4. *Case B* simulation specifications.

Parameter	Value
T_p	2 sec
Q	$C^T C$
R	0.1
p	1.1
N_l	50
γ	15
β	-0.1
h	0.01 sec
$\theta_{ref}(t_0)$	$-20^0 = -0.3491$ rad
$\theta_{ref}(t_f)$	$20^0 = 0.3491$ rad
t_0	0 sec
t_f	12 sec

control and of course may lead the system to instability. This is evident here as well that $N_l = 50$ and $T_p = 2$ [sec] are sufficiently larger values set forth to make the prediction as accurate as possible and to achieve the desired closed loop response of the rotary pendulum system for the defined polynomial type position reference. The choice of $N_l = 50$ is quite practical so as to achieve the desired behavior for rotary inverted pendulum system with a reasonable choice of prediction horizon T_p. This can also be seen from the result of Fig. 9 that the matrix $A(x_m)$ has some eigenvalues in the right half plane as well, thus making the prediction model an unstable one and further increasing the prediction horizon with this matrix or further modifying the parameters within the TV-MPC design will lead the system to instability. The remedy to this problem is the exponential data weighting.

B. CASE-B: WITH EXPONENTIAL DATA WEIGHTING

The proposed TV-MPC has been modified by incorporating an exponential data weighting such that the problem of numerical ill-conditioning is coped. The efficacy, in terms of, robust performance is assessed with the parameters coined in Table 4. The parameters p, N_l, γ and β were chosen and tuned as per the guidelines detailed in [27], [28], [32], [33], and [42].

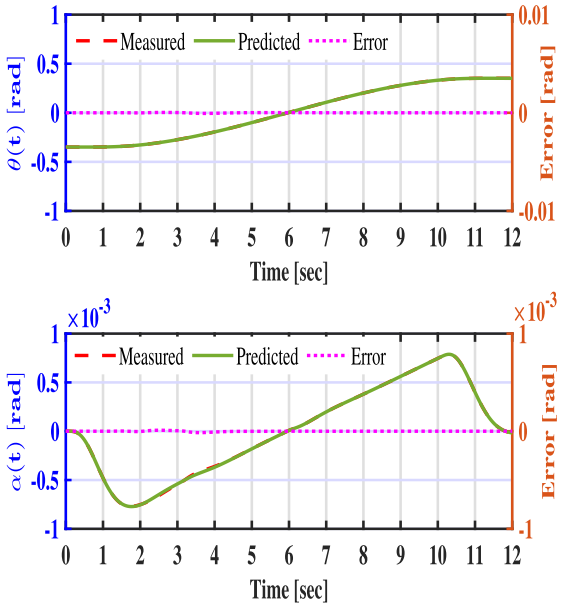

FIGURE 10. Measured versus predicted trajectories for $\theta(t)$ and $\alpha(t)$ with exponential data weighting.

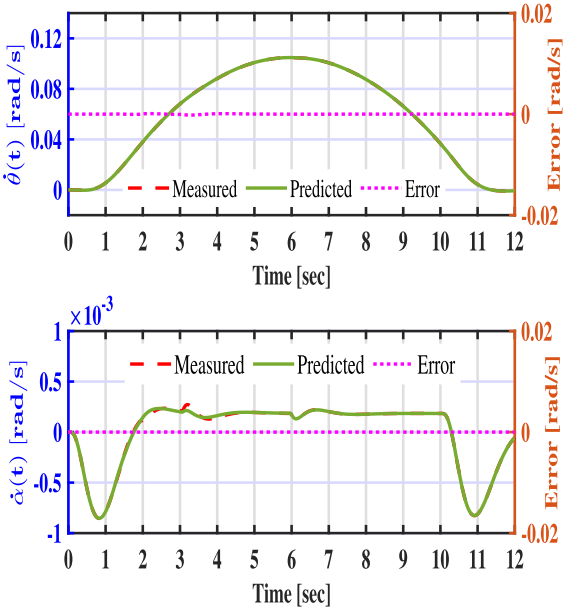

FIGURE 11. Measured versus predicted trajectories for $\dot{\theta}(t)$ and $\dot{\alpha}(t)$ with exponential data weighting.

The predicted and measured states for the pendulum rod angle ($\alpha_{pred}(t)$ and $\alpha_m(t)$, respectively) and position ($\theta_{pred}(t)$ and $\theta_m(t)$, respectively) are shown in Fig. 10 while the respective velocities ($\dot{\alpha}_{pred}(t)$, $\dot{\alpha}_m(t)$, $\dot{\theta}_{pred}(t)$ and $\dot{\theta}_m(t)$) are highlighted in Fig. 11. These results show that all entities/predictions (positions and velocities), generated using the proposed decomposed dynamics, perfectly matches the actual non-decomposed counterpart thus proving accuracy of the algorithm. The results in Fig. 12 demonstrate the tracking performance as the rotary servo arm's position $\theta(t)$ the polynomial type reference.

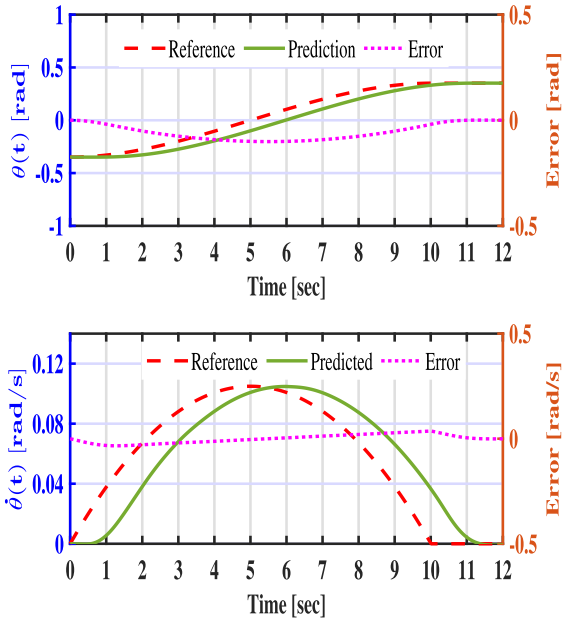

FIGURE 12. Reference versus predicted trajectories for position $\theta_{pred}(t)$ and $\dot{\theta}_{pred}(t)$ with exponential data weighting.

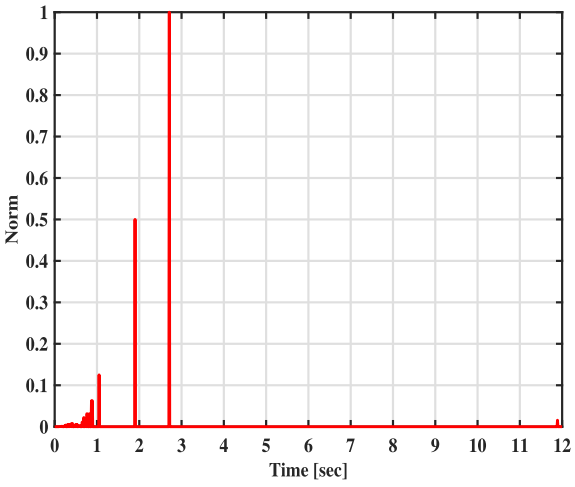

FIGURE 13. Fitness assessment for reference and predicted models with exponential data weighting.

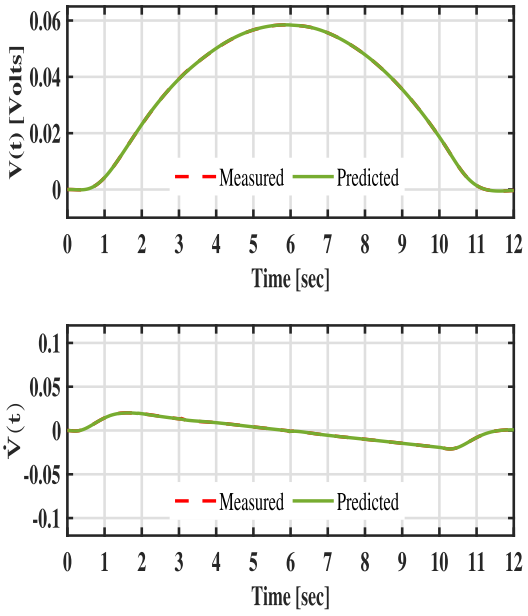

FIGURE 14. Control Trajectories $V(t)$ and $\dot{V}(t)$ with exponential data weighting.

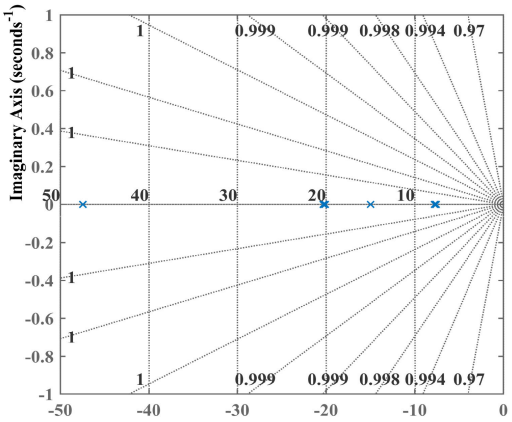

FIGURE 15. Pole-zero map for stability assessment with exponential data weighting.

Remark 1: Here a distinction may be made that, based on the results presented in Figs. 10 and 11, the predicted (θ_{pred}, α_{pred}) and measured (θ_m, α_m) jargons are used synonymously.

The initial and final boundary conditions (-20^0 and $+20^0$) for position $\theta(t)$ are perfectly attained while the tracking errors for both $\theta(t)$ and $\dot{\theta}(t)$, in contrast to the reference polynomial type trajectories, are within the acceptable bounds (within the magnitude of 0.10 rad and 0.10 rad/sec). The fitness assessment, performed the same way as was done for case-A, is considering $\| A_{pred}(x_{pred}) - A_\gamma(x_m) \|_2 < \delta$ where δ is a small positive number defining the fitness bounds. The addition of exponential data weighting improved the condition number $\kappa(\Omega)$, of the Hessian matrix Ω, to be 12.45. This of course is a distinction of the exponential data weighting. Also, the resulting control trajectories ($V_m(t)$, $V_{pred}(t)$ and their respective derivatives) are smooth (see Fig. 14). Moreover, the pole-zero map in Fig. 15 shows that all the eigenvalues for scaled matrix $A_\gamma(x_m)$ are strictly in the left-half complex plane. Thus, making the prediction model stable one and also numerically well-conditioned for a sufficiently large prediction horizon of $T_p = 2$ [sec] and $N_l = 50$. The pole-zero map shows that the time varying scaled matrix $A_\gamma(x_m)$ is strictly Hurwitz for the time from $t_0 = 0$ [sec] to $t_f = 12$ [sec].

VI. CONCLUSION

In this article, a novel, robust and most efficient method toward the design and implementation of continuous-time Time-Varying MPC (TV-MPC) based on dynamics decomposition and Laguerre functions is proposed for the control synthesis of under-actuated mechanical systems. The study in this context is performed and is set confined

to Quanser Inc. Rotary Inverted Pendulum system as an under-actuated benchmark system. A novel and efficient method for the evaluation of the right-hand sides of the nonlinear dynamical Equations Of Motion (EOMs) for Quanser Inc. Rotary Inverted Pendulum system for the control synthesis is devised. Though, the approach is quite extendable and applicable to the wider class of nonlinear systems even if the formulas for their EOMs are very large and complex. This method serves as a most efficient, robust and novel way towards the computation of decomposition of $f(x) = A(x)x$, which is always a key problem in the control synthesis based on the solution of Riccatti equations. The proposed TV-MPC algorithm is based on SDRE solutions. The resulting dynamics decomposition is in state space form with time-varying, state dependent coefficient matrices. The decomposed model is further on incorporated in the TV-MPC model structure and is handled, studied and discussed as two separate sub cases in the context of numerical conditioning, stability and fitness assessment, henceforth. The problem of numerical conditioning is of serious concern when a large prediction horizon is chosen. Moreover, an unstable prediction model with embedded integrator may lead the closed-loop system to the verge of instability in case a large prediction horizon is chosen or any change in design parameters is made within the algorithm at any stage.

The remedy to this issue is exponential data weighting, which provides the guaranteed numerical and closed-loop asymptotic stability with well- conditioned numerical implementation within the underlying TV-MPC algorithm. A concise framework for future control trajectory modeling using the receding horizon principle and Laguerre functions is also discussed from TV-MPC implementation perspective. The simulation results clearly showed that the dynamically decomposed dynamics fits well in accuracy to the actual nonlinear (non-decomposed) model of the Quanser Inc. rotary inverted pendulum model or for any nonlinear dynamical system lying in similar class. The dynamically decomposed model and the actual nonlinear system's model yields almost identical closed-loop responses for the associated TV-MPC control synthesis. It can also be inferred from the simulation results that exponential data weighting adds remarkable improvement to the closed-loop response in terms of accuracy, stability, robustness and performance while tracking the unconventional cubic polynomial type trajectories as a reference position profile for the rotary servo arm's position to balance the pendulum rod.

ACKNOWLEDGMENT

The authors would like to thank Prof. Stefan Streif and Thomas Göhrt at the Automatic Control and Systems Dynamics (ACSD) Laboratory, TU Chemnitz, Germany, for their expert, useful and most valuable suggestions and enthusiastic support during the course of research at TU Chemnitz. The technical support from the University of Sargodha is also acknowledged.

REFERENCES

[1] N. L. Ricker, "Model-predictive control: State of the art," in *Proc. Chem. Process Control (CPC-IV)*, 1991, pp. 271–296.
[2] G. Shi, M. Ma, D. Li, Y. Ding, and K. Y. Lee, "A process-model-free method for model predictive control via a reference model-based proportional-integral-derivative controller with application to a thermal power plant," *Frontiers Control Eng.*, vol. 4, Apr. 2023, Art. no. 1185502.
[3] S. Yu, M. Hirche, Y. Huang, H. Chen, and F. Allgöwer, "Model predictive control for autonomous ground vehicles: A review," *Auto. Intell. Syst.*, vol. 1, no. 1, pp. 1–17, Aug. 2021.
[4] T. Gold, A. Völz, and K. Graichen, "Model predictive interaction control for industrial robots," *IFAC-PapersOnLine*, vol. 53, no. 2, pp. 9891–9898, 2020.
[5] S. Parihar, P. Shah, R. Sekhar, and J. Lagoo, "Model predictive control and its role in biomedical therapeutic automation: A brief review," *Appl. Syst. Innov.*, vol. 5, no. 6, p. 118, Nov. 2022.
[6] E. F. Camacho, D. R. Ramírez, D. Limón, D. M. De La Peña, and T. Alamo, "Model predictive control techniques for hybrid systems," *Annu. Rev. control*, vol. 34, no. 1, pp. 21–31, 2010.
[7] D. Limon, I. Alvarado, T. Alamo, and E. F. Camacho, "On the design of robust tube-based MPC for tracking," *IFAC Proc. Volumes*, vol. 41, no. 2, pp. 15333–15338, 2008.
[8] A. Mesbah, "Stochastic model predictive control: An overview and perspectives for future research," *IEEE Control Syst. Mag.*, vol. 36, no. 6, pp. 30–44, Dec. 2016.
[9] J. Berberich, J. Köhler, M. A. Müller, and F. Allgöwer, "Data-driven model predictive control with stability and robustness guarantees," *IEEE Trans. Autom. Control*, vol. 66, no. 4, pp. 1702–1717, Apr. 2021.
[10] V. Peterka, "Predictor-based self-tuning control," *Automatica*, vol. 20, no. 1, pp. 39–50, Jan. 1984.
[11] A. W. Ordys and D. W. Clarke, "A state-space description for GPC controllers," *Int. J. Syst. Sci.*, vol. 24, no. 9, pp. 1727–1744, Sep. 1993.
[12] K. R. Muske and J. B. Rawlings, "Linear model predictive control of unstable processes," *J. Process Control*, vol. 3, no. 2, pp. 85–96, May 1993.
[13] J. B. Rawlings, "Tutorial overview of model predictive control," *IEEE Control Syst.*, vol. 20, no. 3, pp. 38–52, Jun. 2000.
[14] J. M. Maciejowski, *Predictive Control: With Constraints*. London, U.K.: Pearson, 2002.
[15] C. P. Mracek and J. R. Cloutier, "Control designs for the nonlinear benchmark problem via the state-dependent Riccati equation method," *Int. J. Robust Nonlinear Control*, vol. 8, nos. 4–5, pp. 401–433, Apr. 1998.
[16] E. B. Erdem and A. G. Alleyne, "Design of a class of nonlinear controllers via state dependent Riccati equations," *IEEE Trans. Control Syst. Technol.*, vol. 12, no. 1, pp. 133–137, Jan. 2004.
[17] M. H. Korayem and S. R. Nekoo, "State-dependent differential Riccati equation to track control of time-varying systems with state and control nonlinearities," *ISA Trans.*, vol. 57, pp. 117–135, Jul. 2015.
[18] N. Singh, J. Dubey, and G. Laddha, "Control of pendulum on a cart with state dependent Riccati equations," *World Acad. Sci., Eng. Technol., Int. J. Mech., Aerosp., Ind., Mechtron. Manuf. Eng.*, vol. 2, pp. 759–763, 2008.
[19] K. Belarbi, H. Boumaza, and B. Boutamina, "Nonlinear model predictive control based on state dependent Riccati equation," in *Proc. 15th Int. Conf. Sci. Techn. Autom. Control Comput. Eng. (STA)*, Dec. 2014, pp. 65–69.
[20] Z. Xi and T. Hesketh, "Ball and beam system–nonlinear MPC using Hammerstein model," in *Proc. 2nd IEEE Conf. Ind. Electron. Appl.*, May 2007, pp. 2294–2298.
[21] K. Fruzzetti, A. Palazoğlu, and K. McDonald, "Nolinear model predictive control using Hammerstein models," *J. Process Control*, vol. 7, no. 1, pp. 31–41, 1997.
[22] D. Martinez and F. Ruiz, "Nonlinear model predictive control for a Ball&Beam," in *Proc. IEEE 4th Colombian Workshop Circuits Syst. (CWCAS)*, Nov. 2012, pp. 1–5.
[23] S. J. Norquay, A. Palazoglu, and J. Romagnoli, "Model predictive control based on Wiener models," *Chem. Eng. Sci.*, vol. 53, no. 1, pp. 75–84, Jan. 1998.
[24] M. Ławryńczuk, *Nonlinear Predictive Control Using Wiener Models: Computationally Efficient Approaches for Polynomial and Neural Structures*, vol. 389. Cham, Switzerland: Springer, 2021.
[25] S. Gerksic, D. Juricic, S. Strmcnik, and D. Matko, "Wiener model based nonlinear predictive control," *Int. J. Syst. Sci.*, vol. 31, no. 2, pp. 189–202, 2000.

[26] L. Wang, S. Smith, and C. Chessari, "Continuous-time model predictive control of food extruder," *Control Eng. Pract.*, vol. 16, no. 10, pp. 1173–1183, Oct. 2008.
[27] L. Wang, "Continuous time model predictive control design using orthonormal functions," *Int. J. Control*, vol. 74, no. 16, pp. 1588–1600, Jan. 2001.
[28] L. Wang, *Model Predictive Control System Design and Implementation Using MATLAB*. Cham, Switzerland: Springer, 2009.
[29] L. Wang, "Discrete time model predictive control design using Laguerre functions," in *Proc. Amer. Control Conf.*, Jun. 2001, pp. 2430–2435.
[30] L. Wang and J. A. Rossiter, "Disturbance rejection and set-point tracking of sinusoidal signals using generalized predictive control," in *Proc. 47th IEEE Conf. Decis. Control*, Dec. 2008, pp. 4079–4084.
[31] P. J. Gawthrop, L. Wang, and P. C. Young, "Continuous-time non-minimal state-space design," *Int. J. Control*, vol. 80, no. 10, pp. 1690–1697, Oct. 2007.
[32] P. J. Gawthrop and L. Wang, "Constrained intermittent model predictive control," *Int. J. Control*, vol. 82, no. 6, pp. 1138–1147, Jun. 2009.
[33] L. Wang, "A tutorial on model predictive control: Using a linear velocity-form model," *Develop. Chem. Eng. Mineral Process.*, vol. 12, nos. 5–6, pp. 573–614, Jan. 2004.
[34] L. Wang and P. Gawthrop, "On the estimation of continuous time transfer functions," *Int. J. Control*, vol. 74, no. 9, pp. 889–904, Jan. 2001.
[35] I. M. Mehedi, U. Ansari, A. H. Bajodah, U. M. AL-Saggaf, B. Kada, and M. J. Rawa, "Underactuated rotary inverted pendulum control using robust generalized dynamic inversion," *J. Vibrat. Control*, vol. 26, nos. 23–24, pp. 2210–2220, Dec. 2020.
[36] N. Parks, "Implementing model predictive control on an inverted pendulum," Eng. Des. Project Rep., Swarthmore College, Swarthmore, PA, USA, 2022.
[37] A. M. Lal, Kunjumuhammed, J. Tomy, G. Urmila, M. Sivadas, and A. Mohan, "Stabilization of rotary inverted pendulum using PID controller," in *Proc. 8th Int. Conf. Smart Comput. Commun. (ICSCC)*, Jul. 2021, pp. 376–380.
[38] Q. Inc. (2020). *Rotary Pendulum: User Manual Wrok Book (Instructor)*. Quanser Inc. [Online]. Available: www.quanser.com
[39] D. G. Luenberger and Y. Ye, *Linear and Nonlinear Programming*, vol. 2. Cham, Switzerland: Springer, 1984.
[40] P. J. Gawthrop and L. Wang, "Intermittent predictive control of an inverted pendulum," *Control Eng. Pract.*, vol. 14, no. 11, pp. 1347–1356, Nov. 2006.
[41] B. D. Anderson and J. B. Moore, *Optimal Control: Linear Quadratic Methods*. Chelmsford, MA, USA: Courier Corporation, 2007.
[42] L. Wang, "Use of exponential data weighting in model predictive control design," in *Proc. 40th IEEE Conf. Decis. Control*, Dec. 2001, pp. 4857–4862.

FARRUKH WAHEED received the B.S. degree in electronics from the COMSATS Institute of Information Technology, Islamabad, Pakistan, and the M.S. degree in electronics engineering with a specialization in control systems from Mohammad Ali Jinnah University (MAJU), Islamabad. He is currently pursuing the Ph.D. degree with the Faculty of Mechanical Engineering (FME), Czech Technical University (CTU) in Prague, Czech Republic.

He is an Electronics Engineer by profession. He is a full-time Researcher/Scientist with the IEAP, CTU in Prague. At FME, his work involves the investigation, design, and development of advanced, efficient, and robust nonlinear model predictive control (NMPC) algorithms for under-actuated mechanical systems. At IEAP, he is involved in the research and development of silicon-based pixel detectors for radiation monitoring. He is a member of the Electronics and Software Design Team. His research interests include system design and integration, silicon-based pixel detectors readout solutions for space applications, mechatronics, scientific instrumentation, microcontroller-based system design and integration, vacuum instrumentation, model-based system design, model predictive control, nonlinear model predictive control, robust control, and optimization techniques.

IMRAN KHAN YOUSUFZAI received the B.Sc. degree in electrical engineering from the Federal Urdu University of Arts, Science and Technology, Islamabad, Pakistan, in 2010, the M.Sc. degree in control engineering from Mohammad Ali Jinnah University, Islamabad, in 2012, and the Ph.D. degree in control engineering from the Capital University of Science and Technology, Islamabad, in 2017.

He has more than five years of industrial and teaching experience. He was a Visiting Scholar with The Ohio State University, Columbus, OH, USA. He is currently an Assistant Professor with the Department of Electrical, Electronics and Computer Systems Engineering, College of Engineering and Technology, University of Sargodha, Pakistan. His research interests include the analysis and design of nonlinear control systems, especially sliding mode control, for various industrial applications.

MICHAEL VALÁŠEK was born in Pilsen, in March 1956. He received the degree with a specialization in automated control of technological processes from the Faculty of Mechanical Engineering, Czech Technical University in Prague, in 1980, the Ph.D. degree, in 1984, with a thesis on synthesis of the optimal robot trajectory, and the Dr.Sc. degree, in 1991, with a thesis on theoretical principles of the computational support of engineering work in mechanical engineering.

He became an Associate Professor, in 1992, with a thesis on efficient formulation and implementation of dynamic formalism in computational mechanics. He was appointed as a Full Professor with a lecture on the mechatronics perspective of mechanical engineering, in 1997. He has been the Dean of the Faculty of Mechanical Engineering, since 2018. He is currently a Professor of mechanics with the Faculty of Mechanical Engineering, Czech Technical University in Prague. He has taught courses on mechanics, mechanics of mechanisms, simulation of mechatronic systems, controlled mechanical systems, and mechatronics. He is also active in academic leadership and administration. He has participated in and led many national and international research projects, such as Copernicus, ENCODE, CLOCKWORK, and SIMVIA2. He has published more than 200 scientific articles and several books. His research interests include computational mechanics of multi-body systems, control of nonlinear mechanical systems, mechatronics, robotics, vehicle dynamics, vibration control, and knowledge-based systems for engineering design.

Dr. Valášek has also been involved in various committees and boards at the university and national level. He is a member of the Czech Society for Mechanics, the Czech Society for Cybernetics and Informatics, the International Federation for the Promotion of Mechanism and Machine Science, and the European Association for Structural Dynamics.